Quantum chemical studies of carbon-13 equilibrium fractionation in ion–molecule reactions

Lawrence L. Lohr
Department of Chemistry, University of Michigan, Ann Arbor, Michigan 48109-1055

Ab initio computational quantum chemical methods are used to calculate reduced partition function ratios for all isotopomers of CO, HCO^+, and HOC^+ involving the nuclides ^1H, ^2H (D), ^{12}C, ^{13}C, ^{16}O, and ^{18}O. The ratios are used to calculate equilibrium constants for the reaction pairs HCO^+/CO, HOC^+/CO, and C^+/CO. Both simple proton transfers and more complex isotopic variants involving the breaking and reforming of CO bonds are considered. The probable pathways for the HCO^+/CO and C^+/CO exchange reactions are explored in detail using high-accuracy quantum chemical calculations. It appears most likely that the HCO^+/CO reaction proceeds through exothermic formation of the linear adduct $OCHCO^+$ with $D_{\infty h}$ symmetry. Similarly, the C^+/CO reaction proceeds along a spin-allowed pathway with exothermic formation of the linear adduct COC^+ with $D_{\infty h}$ symmetry. An alternate but higher energy spin-allowed pathway for the C^+/CO reaction passes through a transition state with only C_s symmetry and a locally stable intermediate with C_{2v} symmetry. In the ISM these reactions may proceed by these direct pathways or indirectly through coupled exothermic reaction pairs involving other species to achieve $^{13}C/^{12}C$ isotope exchange. © *1998 American Institute of Physics.* [S0021-9606(98)00719-3]

INTRODUCTION

Experimental and theoretical studies of stable isotope fractionations have played an important role in many aspects of chemistry, including geo- and cosmochemistry, for over half a century, dating from the pioneering studies of Urey,[1] who presented partition functions for the ^{12}C and ^{13}C variants of the carbon species C (diamond), CO, CO_2, $CO_3^=$, HCN, and CN^- and equilibrium constants for their isotope exchange reactions, as well as similar results for species containing other stable isotopes. While Craig[2] discussed the difficulties of applying Urey's methods to fractionation in solid-gas equilibria, many such studies followed, including those by Bottinga,[3–5] and Bottinga and Craig,[6] with an emphasis on equilibria involving C (graphite and diamond), CO_2, $CaCO_3$, and H_2O. These results and others were summarized by Richet *et al.*,[7] while equilibrium isotope effects in general were reviewed by Bigeleisen *et al.*[8] Isotope fractionation in interstellar clouds, including that of C isotopes, was discussed in detail in Watson's review[9] of interstellar molecular reactions. Smith and Adams carried out laboratory studies[10] of fractionation in the reactions of C^+ and HCO^+ with CO, and discussed the implications for interstellar reactions. A representative study[11] of the $^{12}C/^{13}C$ ratio in comets is that based on studies of the CN radical in comet Halley. Further carbon isotope studies include those of CO and C^+ in the Orion molecular cloud.[12] Quite recently C isotope fractionation studies played an important role in developing evidence for life on earth approximately 3800 Myr ago[13] and possibly on Mars.[14]

More relevant to our present study are the many investigations of the relationships between observed isotope fractionations in the ion–molecule reactions occurring in molecular clouds to nuclear abundances in the interstellar medium (ISM). Townes[15] discussed the implications of observed isotopic abundances in interstellar clouds, while Wannier[16] discussed the implications of Watson's[9] proposed chemical models for isotope fractionations for evolution of the ISM. Herbst and Klemperer[17] pioneered model studies of ion–molecule reactions; the latter studies were reviewed in detail by Green.[18] Other reviews include those by Smith and Adams,[19] Kroto,[20] and Dalgarno.[21] In addition, the very recent text by Cowley[2] contains an excellent chapter on isotope effects. Observations of $^{12}C/^{13}C$ ratios in molecular clouds have continued,[23,24] as have model studies[25,26] of the chemical reactions which likely occur in the ISM. A recent review[27] of abundances in the ISM concludes that there most likely is a statistically meaningful dependence of the $^{12}C/^{13}C$ ratios in molecular clouds on the distance of the clouds from the galactic center, with this ratio being smallest (~20–25) near the center, as in the clouds Sgr (Sagittarius) A and B, and increasing with distance to the solar system value of 89.

In our study we have used computational quantum chemical methods to calculate reduced partition function ratios and equilibrium constants for ^{13}C equilibrium fractionations in ion–molecule reactions, with particular emphasis on the HCO^+/CO and HOC^+/CO reaction pairs. We have also explored in detail the structures and energetics of various states of the C_2O^+ ion as may be involved in the isotope exchange reaction between C^+ and CO, proposed by Watson[9] to occur in the ISM.

COMPUTATIONAL METHOD

Electronic structure calculations were made with the GAUSSIAN 94 program[28] at the CISD level (configuration interaction including all single and double excitations from the SCF reference configuration) using initially the split-valence

plus polarization basis set 6-31 G** (six second-order (5 d-type plus 1 s-type) Gaussians for each heavy atom and three p-type for hydrogen) for HCO$^+$ and HOC$^+$, and the basis set 6-31G* (six second-order Gaussians for each heavy atom) for CO and C$_2$O$^+$. This computational level is designated as CISD/6-31G** (or CISD/6-31G* if no H atoms present). Molecular geometries were optimized at this level using analytic gradients, while vibrational frequencies for stationary points were calculated from finite differences of analytic gradients. The energies of a number of possible structures for transition states (saddle points) and intermediates (local minima) for the C$_2$O$^+$ adduct as formed in the isotope exchange reaction between C$^+$ and CO were computed at their CISD/6-31G* optimized geometries using the higher computational level QCISD(T)/6-311G(2df)// CISD/6-31G*. These letters designate quadratic configuration interaction with single, double, and triple electronic excitations, with a triple-zeta basis set augmented by two sets of d-type and one set of f-type polarization functions.

Using the computed molecular structures and vibrational frequencies we next calculate the reduced partition function ratio $Q(^{13}C)/Q(^{12}C)$ for the ^{13}C and ^{12}C isotopic species of a given molecule. (Calculating the ratios of the molecular partition functions for isotopic species implicitly assumes invocation of the Teller–Redlich product rule, with the consequence that the molecular structural information contained in moments of inertia cancels, leaving the reduced ratios dependent only on isotopic changes in harmonic vibrational frequencies.) The reduced partition function ratio is defined as the ratio of the actual partition functions multiplied by the factor $[m(^{13}C)/m(^{12}C)]^{3/2n}$, where n is the number of carbon atoms exchanged; for n of 1 this mass factor equals 1.128 005. (For reactions in which ^{18}O replaces ^{16}O there is similar factor of $[m(^{18}O)/m(^{16}O)]^{3/2} = 1.193\ 728$.) Thus defined, the reduced partition function ratio for exothermic exchange reactions approaches plus infinity as the temperature T approaches zero, but unity as T approached infinity. To obtain these ratios we calculated the molecular partition functions assuming ideal gas behavior for a range of temperatures from $T = 10$ to $T = 1000$ K. All vibrations are assumed to be harmonic and all rotations classical (high-temperature limit). The equilibrium constant K_{eq} expressed in terms of thermodynamic activities $\underline{a}$

$$K_{eq} = [a(^{12}A)a(^{13}B)]/[a(^{13}A)a(^{12}B)] \qquad (1)$$

for a generic isotope exchange reaction

$$^{13}A + {}^{12}B \rightarrow {}^{12}A + {}^{13}B \qquad (2)$$

between species A and B is then given simply by the ratio of the reduced partition function ratio for species B to that for species A.

Fractionation is often expressed[2] in terms of $\delta(^{13}C)$ values which are defined for ^{13}C, ^{12}C mixtures by

$$\delta(^{13}C) = \{[(^{13}C/^{12}C)_{spl} - (^{13}C/^{12}C)_{std}]/(^{13}C/^{12}C)_{std}\} \times 10^3, \qquad (3)$$

where "spl" denotes the sample and "std" the reference standard. The PDB-Chicago standard,[12] based on belemnite fossils of the Peedee, SC, formation, has a value of

TABLE I. Zero-point energies, rotational constants, and vibrational constants.

Species	ZPE[a]	ϑ_{rot}[b]	ϑ_{vib}[c]
CO	1628.5	2.74	3257
^{13}CO	1592.5	2.62	3185
$C^{18}O$	1589.5	2.61	3179
$^{13}C^{18}O$	1552.0	2.49	3104
HCO$^+$	5343.0	2.13	1271 (π), 3332 (σ), 4812 (σ)
H^{13}CO$^+$	5287.0	2.07	1259 (π), 3280 (σ), 4776 (σ)
HC^{18}O$^+$	5296.5	2.04	1268 (π), 3252 (σ), 4805 (σ)
H^{13}C^{18}O$^+$	5239.5	1.98	1256 (π), 3197 (σ), 4770 (σ)
DCO$^+$	4455.0	1.72	1017 (π), 2904 (σ), 3972 (σ)
D^{13}CO$^+$	4395.5	1.69	1002 (π), 2894 (σ), 3893 (σ)
DC^{18}O$^+$	4407.5	1.65	1013 (π), 2856 (σ), 3933 (σ)
D^{13}C^{18}O$^+$	4347.5	1.61	998 (π), 2844 (σ), 3855 (σ)
HOC$^+$	4135.5	2.13	95 (π), 2922 (σ), 5159 (σ)
HO^{13}C$^+$	4102.0	2.04	95 (π), 2856 (σ), 5158 (σ)
H^{18}OC$^+$	4092.5	2.06	94 (π), 2861 (σ), 5136 (σ)
H^{18}O^{13}C$^+$	4058.0	1.97	94 (π), 2793 (σ), 5135 (σ)
DOC$^+$	3403.5	1.81	69 (π), 2814 (σ), 3855 (σ)
DO^{13}C$^+$	3369.5	1.74	69 (π), 2752 (σ), 3849 (σ)
D^{18}OC$^+$	3359.5	1.77	69 (π), 2775 (σ), 3806 (σ)
D^{18}O^{13}C$^+$	3325.0	1.69	69 (π), 2711 (σ), 3801 (σ)

[a]Zero-point energy in K computed at optimized CISD/6-31G** level.
[b]Rotational constants in K computed at optimized CISD/6-31G** level.
[c]Vibrational constants in K computed at optimized CISD/6-31G** level.

$(^{13}C/^{12}C)_{std} = 0.011\ 24$, corresponding to which the $^{12}C/^{13}C$ ratio is 88.968 and the atom fraction of ^{13}C is 0.011 12. Taking the activity for a given isotopic species to be proportional to its atomic concentration, an equilibrium constant may be rewritten as

$$K_{eq} = (^{13}C/^{12}C)_B/(^{13}C/^{12}C)_A = [1 + 10^{-3}\delta(B)]/[1 + 10^{-3}\delta(A)], \qquad (4)$$

where $\delta(B)$ and $\delta(A)$ denote the $\delta(^{13}C)$ values for the ^{13}C containing product and reactant species, respectively. Note that the reference ratio $(^{13}C/^{12}C)_{std}$ in Eq. (3) does not appear in Eq. (4), and that $\delta(B)$ and $\delta(A)$ are not uniquely determined by the value of K_{eq}.

RESULTS AND DISCUSSION

Zero-point energies, spectroscopic constants, and partition functions

In Table I we list the computed zero-point energies in K together with computed rotational constants and harmonic vibrational frequencies, also expressed in K, for the various isotopomers of CO, HCO$^+$, and HOC$^+$. We have chosen to express these constants in temperature units rather than wave numbers as our applications are primarily statistical thermodynamic rather than spectroscopic. In Tables II, III, and IV we list as a function of temperature reduced partition function ratios $Q(^{13}C)/Q(^{12}C)$ for CO, HCO$^+$, and HOC$^+$, respectively.

Equilibrium constants K_{eq} as a function of temperature for isotope exchange reactions having the form of the generic reaction (2) are given by the quotient of the appropriate pair of reduced partition function ratios as given in Tables II–IV. If the species A is atomic carbon (charged or neutral), the

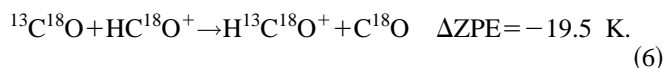TABLE II. Reduced partition function ratios[a,b] $Q(^{13}C)/Q(^{12}C)$ for CO.

$T(K)$	$^{13}CO/CO$	$^{13}C^{18}O/C^{18}O$	$^{13}CO/C^{18}O$	$^{13}C^{18}O/CO$
10	36.90	40.41	0.739	2016
25	4.178	4.329	0.887	20.38
50	2.021	2.056	0.942	4.407
100	1.406	1.417	0.972	2.049
200	1.172	1.176	0.987	1.400
300	1.103	1.106	0.992	1.230
400	1.071	1.072	0.994	1.154
600	1.039	1.040	0.997	1.084
800	1.025	1.025	0.998	1.052
1000	1.017	1.017	0.999	1.036

[a]All values calculated at optimized CISD/6-31G** level.
[b]The reduction factors are $[m(^{13}C)/m(^{12}C)]^{3/2}=1.128\,005$ and $[m(^{18}O)/m(^{16}O)]^{3/2}=1.193\,728$.
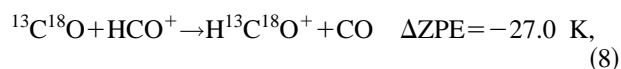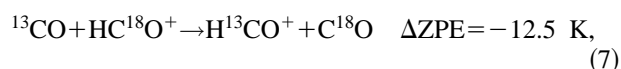
equilibrium constants are given directly by the reduced partition function ratio for species B as that for the atomic species is taken to be unity. Values of $\delta(^{13}C)$ for any exchange reaction may be obtained given some assumption about the relationship of δ for species B to that for species A.

HCO⁺/CO

In Table V we list K_{eq} values for isotope exchange reactions involving the species HCO⁺ and CO, displayed with their ΔZPE values in K, the latter corresponding to ΔU values at 0 K. The first two are

$$^{13}CO+HCO^+\rightarrow H^{13}CO^++CO \quad \Delta ZPE=-20.0 \text{ K,} \tag{5}$$

$$^{13}C^{18}O+HC^{18}O^+\rightarrow H^{13}C^{18}O^++C^{18}O \quad \Delta ZPE=-19.5 \text{ K.} \tag{6}$$

(Unlabeled atoms are understood to represent the most abundant isotopes, namely ^1H, ^{12}C, and ^{16}O.) Other isotopic variants of the above exchange reactions include simple proton transfers which are in effect exchanges of two isotopes, namely

$$^{13}CO+HC^{18}O^+\rightarrow H^{13}CO^++C^{18}O \quad \Delta ZPE=-12.5 \text{ K,} \tag{7}$$

$$^{13}C^{18}O+HCO^+\rightarrow H^{13}C^{18}O^++CO \quad \Delta ZPE=-27.0 \text{ K,} \tag{8}$$

TABLE III. Reduced partition function ratios[a,b] $Q(^{13}C)/Q(^{12}C)$ for HCO⁺ and HOC⁺.

$T(K)$	$H^{13}CO^+/$ HCO^+	$H^{13}C^{18}O^+/$ $HC^{18}O^+$	$HO^{13}C^+/$ HOC^+	$H^{18}O^{13}C^+/$ $H^{18}OC^+$
10	246.8	268.6	27.76	29.99
25	8.798	9.131	3.718	3.832
50	2.905	2.958	1.902	1.930
100	1.669	1.683	1.360	1.369
200	1.266	1.270	1.150	1.153
300	1.155	1.158	1.088	1.089
400	1.105	1.106	1.058	1.058
600	1.058	1.059	1.029	1.030
800	1.037	1.037	1.016	1.016
1000	1.026	1.026	1.010	1.010

[a]All values calculated at optimized CISD/6-31G** level.
[b]The reduction factor is $[m(^{13}C)/m(^{12}C)]^{3/2}=1.128\,005$.

TABLE IV. Reduced partition function ratios[a,b] $Q(^{13}C)/Q(^{12}C)$ for DCO⁺ and DOC⁺.

$T(K)$	$D^{13}CO^+/$ DCO^+	$D^{13}C^{18}O^+/$ $DC^{18}O^+$	$DO^{13}C^+/$ DOC^+	$D^{18}O^{13}C^+/$ $D^{18}OC^+$
10	360.8	395.9	28.51	30.68
25	10.21	10.59	3.751	3.859
50	3.113	3.168	1.907	1.933
100	1.718	1.733	1.359	1.369
200	1.278	1.282	1.148	1.150
300	1.160	1.163	1.085	1.086
400	1.108	1.109	1.055	1.055
600	1.060	1.060	1.026	1.026
800	1.038	1.038	1.013	1.013
1000	1.026	1.026	1.007	1.006

[a]All values calculated at optimized CISD/6-31G** level.
[b]The reduction factor is $[m(^{13}C)/m(^{12}C)]^{3/2}=1.128\,005$.

as well as reactions which are not simple proton transfers but instead involve breaking and reforming CO bonds to achieve exchange of a single isotope, namely,

$$^{13}CO+HC^{18}O^+\rightarrow H^{13}C^{18}O^++CO \quad \Delta ZPE=-21.0 \text{ K,} \tag{9}$$

$$^{13}C^{18}O+HCO^+\rightarrow H^{13}CO^++C^{18}O \quad \Delta ZPE=-18.5 \text{ K.} \tag{10}$$
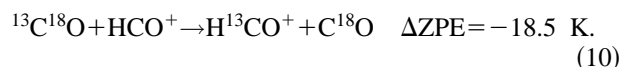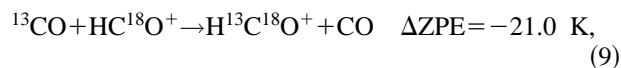
Equilibrium constants for reactions (5), (6), (9), and (10) differ negligibly as their ΔZPE values differ negligibly. Reaction (7), which involves one heavy isotope in each reactant and product species, is the least exothermic of the set of six reactions, while reaction (8), which concentrates both heavy isotopes in the product species $H^{13}C^{18}O^+$, is the most exothermic. [The equilibrium constants for all of the above reactions except Eqs. (7) and (8) are obtained as quotients of reduced partition function ratios from Tables III and IV; the mixed CO ratios needed for Eqs. (7) and (8) are included in Table II, but the mixed ratios for HCO⁺ are not tabulated.] The HCO⁺/CO exchange reactions may be exothermic without having ^{13}CO or $^{13}C^{18}O$ as a reactant; subtracting Eq. (7) from Eqs. (9) or (10) from Eq. (8) yields

$$C^{18}O+H^{13}CO^+\rightarrow H^{13}C^{18}O^++CO \quad \Delta ZPE=-8.5 \text{ K.} \tag{11}$$
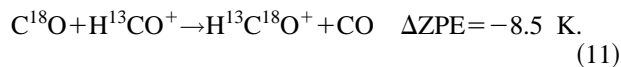
Another exothermic variant is obtained by subtracting Eq. (7) from Eqs. (10) or (9) from Eq. (8), yielding

$$^{13}C^{18}O+HCO^+\rightarrow HC^{18}O^++^{13}CO \quad \Delta ZPE=-6.0 \text{ K.} \tag{12}$$
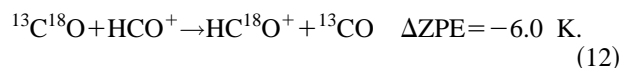
We do not tabulate the K_{eq} values for the slightly exothermic reactions (11) and (12), as they may be readily obtained by combining tabulated values.

While at temperatures of say, 10 to 50 K, ΔG° values for isotope exchange reactions are approximated well by zero-point energy differences (ΔZPE's), so that equilibrium constants are approximately $\exp(-\Delta ZPE/RT)$, at temperatures of several hundred K the ΔG° values are considerably smaller in magnitude than the ΔZPE's. For reaction (5) ΔZPE is -158 J mol^{-1}, while ΔG° at 500 K is -96 J mol^{-1}; K_{eq} is 1.023 vs 1.039 if approximated as $\exp(-\Delta ZPE/RT)$. The difference appears slight, but the deviations from unity, to which equilibrium fractionations are closely related, are significantly different.

TABLE V. Isotope exchange equilibrium constants for HCO$^+$/CO reactions.[a]

T(K)	HCO$^+$/^{13}CO H^{13}CO$^+$/CO	HC^{18}O$^+$/^{13}C^{18}O H^{13}C^{18}O$^+$/C^{18}O	HC^{18}O$^+$/^{13}CO H^{13}CO$^+$/C^{18}O	HCO$^+$/^{13}C^{18}O H^{13}C^{18}O$^+$/CO	HC^{18}O$^+$/^{13}CO H^{13}C^{18}O$^+$/CO	HCO$^+$/^{13}C^{18}O H^{13}CO$^+$/C^{18}O
10	6.690	6.648	3.327	13.37	7.281	6.109
25	2.106	2.109	1.605	2.768	2.186	2.032
50	1.438	1.438	1.254	1.643	1.464	1.413
100	1.187	1.188	1.111	1.266	1.198	1.178
150	1.114	1.115	1.070	1.160	1.120	1.109
200	1.080	1.080	1.049	1.111	1.084	1.076
300	1.047	1.047	1.029	1.065	1.049	1.045
400	1.032	1.032	1.019	1.044	1.033	1.030
500	1.023	1.023	1.014	1.032	1.024	1.022
600	1.018	1.018	1.011	1.025	1.019	1.018
700	1.014	1.014	1.009	1.020	1.015	1.014
800	1.012	1.012	1.007	1.016	1.012	1.012
900	1.010	1.010	1.006	1.014	1.010	1.010
1000	1.008	1.008	1.005	1.012	1.009	1.008
ΔZPE[b]	-20.0	-19.5	-12.5	-27.0	-21.0	-18.5

[a]The first line denotes reactants, the second denotes products. The reactions are given by Eqs. (5)–(10).
[b]Zero-point energy changes in K.

In their laboratory SIFT (selected ion flow tube) studies of the reactions of HCO$^+$ with CO, Smith and Adams[10] obtained K_{eq} values for reaction (5) of 1.17, 1.07, 1.04, and 1.00 for $T=80$, 200, 300, and 510 K, respectively, in reasonable agreement with our computed values of 1.187, 1.080, 1.047, and 1.023 for $T=100$, 200, 300, and 500 K, respectively. They also noted that since reactions such as Eqs. (7) and (9) involve the same reactants [as does also the endothermic reverse of Eq. (12)], single reversible reactions cannot be cleanly studied for these mixed (^{12}C, ^{13}C, ^{16}O, ^{18}O) systems. Similarly, the endothermic reverses of Eqs. (8), (9), and (11) have identical reactants. They do report that the appearance of channel (9) is about 10% of that for the less exothermic (by almost a factor of 2) channel (7), but as noted above, (7) is a simple proton transfer, while (9) involves breaking and reforming the CO bonds, which undoubtedly accounts for the greater importance of Eq. (7) compared to Eq. (9).

A striking result of these SIFT studies[10] of the HCO$^+$/CO exchange reaction is the observed decrease in both the forward and reverse rate constants as the temperature is increased from 80 to 510 K, a result strongly suggestive of a reaction pathway involving exothermic complex formation. We have located a centrosymmetric linear saddle point with connectivity OCHCO on the five-atom potential energy surface for CO+HCO$^+$. At the optimized CISD/6-31G** level the CO and CH separations are 1.115 and 1.382 Å, respectively, with the only imaginary vibrational wave number being $1039i$ cm^{-1} for an antisymmetric σ_u stretching mode. The energy of this possible transition state structure for proton transfer between HCO$^+$ and CO, and hence for ^{13}C/^{12}C isotope exchange, is -46.0 kJ mol^{-1} relative to that of the reactants at the higher QCISD(T)/6-311g(2df)//CISD/6-31G** level; the zero-point energy change for formation of this transition state from HCO$^+$ and ^{13}CO is -4.1 kJ mol^{-1} at the CISD/6-31G** level, giving a total exothermicity of -50.1 kJ mol^{-1}. The imaginary σ_u vibrational frequency in turn implies that a linear structure with unequal CH separa-

tions lies at a still lower energy, thus supporting the suggestion of exothermic complex formation at least for those HCO$^+$/CO exchanges which may occur by proton transfer rather than by breaking and reforming CO bonds. In the next section we discuss in greater detail complex formation and the observation[10] of similar anti-Arrhenius behavior in the reaction of C$^+$ with CO.

Equilibrium constants for the deuterium counterpart of Eq. (5), namely

$$^{13}\text{CO}+\text{DCO}^+\rightarrow\text{D}^{13}\text{CO}^++\text{CO} \quad \Delta\text{ZPE}=-23.0 \text{ K} \quad (13)$$

are given in Table VI. The values are slightly higher than their proton counterparts due to the slightly higher exothermicity of the deuterium reaction. Values for the ^{18}O variant of Eq. (13) are not sufficiently different from those for Eq. (13) to warrant tabulation.

TABLE VI. Isotope exchange equilibrium constants for DCO$^+$/CO, HOC$^+$/CO, and DOC$^+$/CO reactions.[a]

T(K)	DCO$^+$/^{13}CO D^{13}CO$^+$/CO	HO^{13}C$^+$/CO HOC$^+$/^{13}CO	DO^{13}C$^+$/CO DOC$^+$/^{13}CO
10	9.780	1.329	1.294
25	2.445	1.124	1.114
50	1.540	1.062	1.060
100	1.222	1.034	1.034
150	1.132	1.024	1.026
200	1.090	1.019	1.021
300	1.052	1.015	1.017
400	1.035	1.012	1.015
500	1.025	1.011	1.014
600	1.019	1.010	1.013
700	1.016	1.009	1.012
800	1.013	1.008	1.011
900	1.010	1.008	1.010
1000	1.009	1.007	1.010
ΔZPE[b]	-23.0	-2.5	-2.0

[a]The first line denotes reactants, the second denotes products. The reactions are given by Eqs. (13)–(15).
[b]Zero-point energy changes in K.

HOC$^+$/CO

An important isomer of HCO$^+$ is HOC$^+$, the analog of hydrogen isocyanide. Measurements of the millimeter-wave transitions of HOC$^+$ in dense molecular clouds have recently been made[29] and used to obtain [HCO$^+$]/[HOC$^+$] ratios. At the optimized CISD/6-31G** level this isomer lies higher in electronic energy by 150.9 kJ mol^{-1} or 18,150 K than the more stable HCO$^+$ isomer. The zero-point energy difference lowers this by 1208 K for ^{12}C and by 1185 K for ^{13}C (Table I). Table VI lists values of the equilibrium constant for the exchange reaction

$$CO + HO^{13}C^+ \rightarrow HOC^+ + {}^{13}CO \quad \Delta ZPE = -2.5 \text{ K} \quad (14)$$

and its deuterium counterpart

$$CO + DO^{13}C^+ \rightarrow DOC^+ + {}^{13}CO \quad \Delta ZPE = -2.0 \text{ K}. \quad (15)$$

The exothermicities are small, but note that the direction of the reactions is the opposite of that for HCO$^+$/CO exchange, namely that there is a slight preference for ^{13}C being in CO rather than in HOC$^+$.

The reaction of C$^+$ and CO

Watson[9] proposed that significant chemical fractionation of C isotopes in the ISM might occur via the reaction

$$^{13}C^+ + CO \rightarrow C^+ + {}^{13}CO, \quad (16)$$

if sufficiently large amounts of C$^+$ were present. Given the significance of this proposal we have considered possible pathways for this isotope exchange. First, it may well be that such exchanges, assuming that they occur in the ISM, take place indirectly via exothermic reaction pairs such as

$$C^+ + OH \rightarrow CO + H^+, \quad (17)$$

$$He^+ + CO \rightarrow C^+ + O + He, \quad (18)$$

just as exchange between CO and HCO$^+$ may occur via the exothermic reaction pair

$$H_3^+ + CO \rightarrow H_2 + HCO^+, \quad (19)$$

$$HCO^+ + e^- \rightarrow H + CO. \quad (20)$$

Reaction (19) presumably proceeds through the adduct H$_2\cdots$HCO$^+$, which has been studied[30] by ir spectroscopy; the more stable[30] protonated formaldehyde isomer H$_2$COH$^+$ does not lead to HCO$^+$ production. Different rate constants for different C isotopes in a reaction pair can lead to chemical fractionation, although such differences are expected to be small for exothermic pairs such as Eqs. (19) and (20). Alternatively reaction (16) may proceed directly, via a C$_2$O$^+$ adduct, as is presumably the case in the laboratory SIFT studies of Smith and Adams.[10] They found K_{eq} values, defined as the ratio k_f/k_r of forward and reverse rate constants, for reaction (16) to be 1.66, 1.20, 1.14, and 1.04 at $T = 80$, 200, 300, and 510 K, respectively; from the temperature dependence of K_{eq} they extracted a ΔE value of -40 ± 6 K. Our calculated equilibrium constants for Eq. (16) are equal to the reduced partition function ratios for CO as given in Table II; the values are 1.406, 1.172, 1.103, and 1.052 for temperatures of 100, 200, 300, and 500 K, respectively. A

striking result was their finding that the individual rate constants decreased with rising temperature, k_f by a factor of 2.6 as T increased from 80 to 510 K, and k_r by a factor of 1.6. They interpreted this anti-Arrhenius behavior as evidence for adduct formation, which is the aspect of this reaction we explore next.

There have been a number of computational quantum chemical studies of C$_2$O$^+$. First, HF/DZ (double-zeta) structures with $C_{\infty v}$ symmetry have been reported[31] for linear $^2\Pi$ states with both CCO and COC connectivities, the latter with unequal CO bond lengths, as well as for a presumed linear saddle point structure with $D_{\infty h}$ symmetry. Results have also been reported at various higher levels of computation for the two linear $^2\Pi$ states,[32,33] for linear $^2\Sigma^-$ and $^4\Sigma^-$ states with CCO connectivity,[34] and for a triangular (C_{2v} symmetry) $^4A_2$ transition state.[34] A state should meet two requirements for it to serve as an intermediate for reaction (14), first, that the 2 C atoms should occupy equivalent positions in the structure (thus excluding the linear CCO$^+$ forms and the noncentrosymmetric COC$^+$ form), and second, that the electronic state should be a spin doublet. The latter requirement follows from the spin state of C$^+$ being a doublet (^2P) and that of CO a singlet, so that exchange proceeding through a quartet intermediate to doublet products would involve two curve crossings and thus be inefficient although not precluded. The only reported structure satisfying these requirements is the centrosymmetric COC$^+$ saddle point,[31] with a HF/DZ energy approximately 32 kJ mol^{-1} above that of the C$^+$ and CO reactants.

We have located a total of 9 stationary points, 5 corresponding to spin doublets and 4 to spin quartets, on the C$_2$O$^+$ surface at the CISD/6-31G* level. Vibrational frequencies were calculated at this level from finite differences of analytic first derivatives, and then the energies were recalculated at the higher QCISD(T)/6-311G(2df) level using the CISD/6-31G* geometries. The energies and structures are summarized in Tables VII and VIII, respectively. We first discuss the spin doublets as they may be derived from the ground states of C$^+$ and CO. The lowest energy spin doublet is the previously reported[31-33] linear $^2\Pi$ state with connectivity CCO$^+$. The CC distance is long (1.600 Å), the CO distance short (1.094 Å), so the structure clearly represents an adduct of C$^+$ and an only slightly perturbed CO. The energy is -250.7 kJ mol^{-1} relative to C$^+$+CO at the QCISD(T)/6-311G(2df)//CISD/6-31G* level. However, this structure cannot account for the exchange of C atoms between C$^+$ and CO. By contrast the linear $^2\Pi$ state with connectivity COC$^+$ may, as it is associated with a symmetric double-well potential energy function. The $^2\Pi_g$ state of the centrosymmetric $D_{\infty h}$ structure has an energy of -84.4 kJ mol^{-1} relative to C$^+$+CO at the QCISD(T)/6-311G(2df)//CISD/6-31G* level, and is unstable with respect to the antisymmetric stretching mode leading to the $^2\Pi$ state of a noncentrosymmetric $C_{\infty v}$ structure having an energy of -102.5 kJ mol^{-1}. Figure 1 shows a schematic potential energy curve of the exothermic formation of this linear adduct; the relative energy values include zero-point energies at the CISD/6-31G* level as appropriate to the presence of one ^{13}C in the reaction. With this inclusion the $D_{\infty h}$

TABLE VII. *Ab initio* energies and energy differences[a] for the C_2O^+/C^++CO exchange reaction.

Symmetry (Term)	CISD/6-31G*	QCISD(T)/6-311G($2df$)	ZPE(^{12}C)	[b]ZPE(^{13}C)[c]
$C_{\infty v}(^2\Pi)$, CCO$^+$	−150.428 22	−150.610 51	0.008 51	0.008 33,0.008 47
	(−168.4)	(−250.7)	(+8.8)	(+8.6, +9.0)
$C_{\infty v}(^2\Pi)$, COC$^+$	−150.384 73	−150.554 05	0.005 98	0.005 87,0.005 96
	(−54.3)	(−102.5)	(+2.2)	(+2.2, +2.4)
$D_{\infty h}(^2\Pi_g)$, COC$^+$	−150.370 09	−150.547 16	0.003 85	0.003 79
	(−15.8)	(−84.4)	(−3.4)	(−3.3)
$C_{2v}(^2A_1)$	−150.363 71	−150.543 96	0.005 98	0.005 90
	(+0.9)	(−76.0)	(+2.2)	(+2.3)
$C_s(^2A')$	−150.356 94	−150.537 37	0.005 01	0.004 99,0.004 92
	(+18.6)	(−58.7)	(−0.4)	(−0.1, −0.3)
$C_{\infty v}(^4\Sigma^-)$, CCO$^+$	−150.432 12	−150.601 98	0.010 42	0.010 22,0.010 33
	(−178.7)	(−228.3)	(+13.8)	(+13.6, +13.9)
$C_s(^4A'')$	−150.309 27	−150.483 96	0.007 45	0.007 32,0.007 37
	(+143.8)	(+81.5)	(+6.0)	(+6.0, +6.1)
$C_{2v}(^4A_2)$	−150.308 49	−150.484 38	0.011 83	0.011 65
	(+145.9)	(+80.4)	(+17.5)	(+17.4)
$D_{\infty h}(^4\Sigma_u^-)$, COC$^+$	−150.261 89	−150.465 00	0.007 76	0.007 66
	(+268.2)	(+131.2)	(+6.8)	(+6.9)
$C^+(^2P)+CO$	−150.364 06	−150.515 01	0.005 16	0.005 04
	(0)	(0)	(0)	(0)

[a]Energies in hartrees and energy differences (in parentheses) in kJ mol^{-1}, all at optimized CISD/6-31G* geometries. The $D_{\infty h}(^2\Pi_g)$ and $C_s(^2A')$ structures are saddle points, the others local minima at this level.
[b]Zero-point energy of pure ^{12}C species.
[c]Zero-point energy of mixed ^{13}C, ^{12}C species; the first value for C_s symmetry is for long bond to ^{13}C, the second is for long bond to ^{12}C. The first $C_{\infty v}$ entries are for terminal ^{12}C, the second for terminal ^{13}C. The C$^+$+CO entry is for ^{12}C$^+$+^{13}CO.

and $C_{\infty v}$ structures lie at −77.8 and −100.4 kJ mol^{-1}, respectively, relative to C$^+$+CO reactants. Our result confirms the conjecture[31] that this structure, which has an energy above that of the C$^+$ and CO reactants at the SCF level of computations, would have an energy below that of reactants at a sufficiently high level of computation. Thus exchange of C atoms between C$^+$ and CO may well occur via a spin-allowed pathway through the centrosymmetric COC$^+$ saddle point.

Another possible spin-allowed pathway for exchange of C atoms between C$^+$ and CO involves the electronic state $^2A_1$ for a structure with C_{2v} symmetry. This structure is a local minimum with an energy of −76.0 kJ mol^{-1} relative to that of C$^+$ and CO at the QCISD(T)/6-311G($2df$)// CISD/6-31G* level. We have also located a saddle point with symmetry C_s; the electronic state is $^2A'$, with an electronic energy 17.3 kJ mol^{-1} above that of the C_{2v} local mini-

mum, or −58.7 kJ mol^{-1} relative to C$^+$+CO. The C_s structure is characterized by one long CO bond of 1.482 Å, one short bond of 1.218 Å, a COC angle of 88.5°, and a single imaginary a' vibrational wave number with magnitude 603 cm^{-1} at the CISD/6-31G* level. These two spin doublet structures lie on the same potential energy surface, namely, one correlated to the $^2\Sigma^+$ state of collinear COC$^+$ rather than

TABLE VIII. *Ab initio* structural parameters[a] for C_2O^+.

Symmetry (Term)	C_1–O	C_2–O	C_1–C_2
$C_{\infty v}(^2\Pi)$, CCO$^+$	1.118	⋯	1.566
$C_{\infty v}(^2\Pi)$, COC$^+$	1.162	1.659	⋯
$D_{\infty h}(^2\Pi_g)$, COC$^+$	1.261	1.261	⋯
$C_{2v}(^2A_1)$	1.314	1.314	1.641
$C_s(^2A')$	1.218	1.482	1.894
$C_{\infty v}(^4\Sigma^-)$, CCO$^+$	1.128	⋯	1.110
$C_s(^4A'')$	1.269	1.539	1.359
$C_{2v}(^4A_2)$	1.394	1.394	1.319
$D_{\infty h}(^4\Sigma_u^-)$, COC$^+$	1.242	1.242	⋯

[a]Bond distances in Ångstroms from optimized CISD/6-31G* geometries. The $D_{\infty h}(^2\Pi_g)$COC$^+$ and $C_s(^2A')$ structures are saddle points, the others local minima. The computed distance for CO is 1.136 Å.
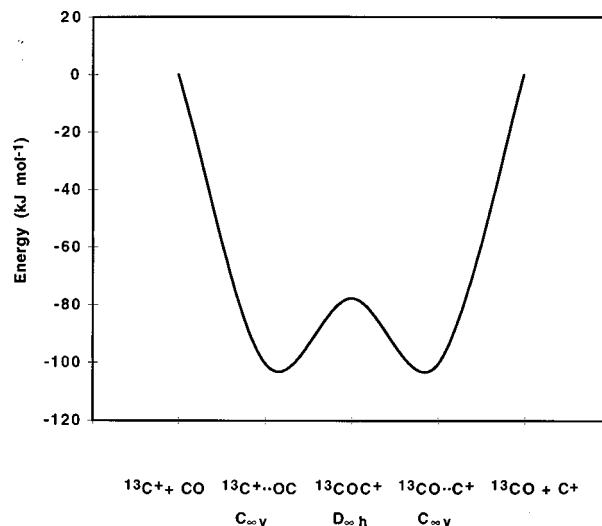

FIG. 1. Schematic potential energy curve showing exothermic formation of the linear adduct COC$^+$ in the C$^+$/CO isotope exchange reaction. All energies (in kJ mol^{-1}) are relative to that of the ^{13}C$^+$ and CO reactants, and are a combination of electronic energies at the QCISD(T)/6-311G($2df$)// CISD/6-31G* level and zero-point vibrational energies at the CISD/6-31G* level. The overall energy change of −0.3 kJ mol^{-1} is insignificant on the scale of the diagram. Exothermic formation of the linear adduct OCHCO$^+$ in the HCO$^+$/CO exchange reaction may be described by a similar diagram.

to the $^2\Pi$ state. [The latter gives rise to $^2A_2$ and $^2B_1$ (or $^2B_2$) states in C_{2v} symmetry, but not $^2A_1$.] Thus a second possible spin-allowed pathway for C isotope exchange between C^+ and CO might be that passing through a pair of C_s saddle points separated by a C_{2v} local minimum. The highest energy along such a pathway is higher by 25.7 kJ mol^{-1} at the QCISD(T)/6-311G($2df$)//CISD/6-31G* level (Table VII) than that along the pathway passing through the centrosymmetric COC$^+$ saddle point, but still below (by 58.7 kJ mol^{-1}) that of the separated reactants.

Even allowing for some appreciable error in the computation of the energies of C_2O^+ structures relative to the energies of C^+ and CO, we conclude that there no barrier to isotope exchange if reaction (19) proceeds via either of the above spin-allowed pathways, namely, either through the COC$^+$ saddle point with $D_{\infty h}$ symmetry or through the C_2O^+ local minimum with C_{2v} symmetry. The COC$^+$ $^2\Pi$ state may be interpreted as arising from the $^2\Pi$ components of the atomic ^2P term for C^+; these have an empty p_σ orbital which serves as an electron acceptor site from a filled σ orbital at the O end of CO, thus accounting for the linearity of this state of the adduct. The linear but noncentrosymmetric structure of this state is quite unusual; rare indeed are triatomic molecules, linear or bent, neutral or charged, of the formula ABA, with B as the central atom, but with AB bonds of unequal length. By contrast, the $^2A'$ (C_s) or $^2A_1$ (C_{2v}) state is nonlinear, as it is derived from the $^2\Sigma^+$ component of the atomic ^2P term for C^+ and thus has an electron in the C^+ p_σ orbital.

We have also considered spin quartet states of C_2O^+. First, we refined the CISD/6-31G*//HF/6-31G* calculations of Cao and Tian[34] on the linear $^4\Sigma^-$ local minimum and the isosceles triangular $^4A_2$ transition state with C_{2v} symmetry. Our optimized CISD/6-31G* geometries (Table VIII) differ slightly but not significantly from the reported HF/6-31G* geometries; for the linear quartet the CC distance is 1.356 Å and the CO distance is 1.128 Å, while for the triangular transition state the CC distance is 1.394 Å, the CO distance is 1.319 Å, and the COC angle is 56.5°. Although the $^4A_2$ state corresponds to a saddle point at the HF/6-31G* level, with imaginary b_2 wave number of $1415i$ cm^{-1}, it corresponds to a local minimum at the optimized CISD/6-31G* level, with real b_2 wave number of 2242 cm^{-1}. While the energy of the linear quartet is quite low, namely, -228.3 kJ mol^{-1} relative to C^+ and CO at the QCISD(T)/6-311G($2df$)//CISD/6-31G* level, the connectivity CCO does not lead to an exchange of C atoms. The triangular structure with C_{2v} symmetry, which has equivalent C atoms and hence could lie on an exchange pathway, has a very high energy, namely $+80.4$ kJ mol^{-1} at the same level. This high energy, plus the two electronic spin changes needed to pass from spin doublet reactants through this quartet intermediate to doublet products, precludes this structure as a likely route to isotope exchange between C^+ and CO.

We did locate two additional spin quartet local minima, the first being a $^4A''$ state with a nonlinear structure of only C_s symmetry, unequal CO bond distances of 1.269 and 1.539 Å, a COC bond angle of 56.9° at the CISD/6-31G* level, and an energy of $+81.5$ kJ mol^{-1} relative to C^+ and CO at

the QCISD(T)/6-311G($2df$)//CISD/6-31G* level. The energy of this structure is close to that of the isosceles triangular $^4A_2$ state at this as well as at lower computational levels. Indeed the two structures represent two points on the same quartet hypersurface, both being local minima at the CISD/6-31G* level, although the higher symmetry C_{2v} structure is a saddle point at the lower HF/6-31G* level. Finally at a very high energy of $+131.2$ kJ mol^{-1} relative to C^+ and CO at the QCISD(T)/6-311G($2df$)//CISD/6-31G* level there is a $^4\Sigma_u^-$ state of a centrosymmetric structure with connectivity C–O–C ($D_{\infty h}$ symmetry) and CO distances of 1.242 Å at the CISD/6-31G* level. As we have been unable to locate any spin quartet structure for C_2O^+ having equivalent C atom positions and an energy comparable to or below that of C^+ and CO, we conclude that C atom exchange takes place along an allowed spin doublet pathway involving exothermic formation of the adduct C_2O^+, thus accounting for the observed anti-Arrhenius behavior of the rate constants.

SUMMARY

We have employed *ab initio* computational quantum chemical methods to calculate reduced partition function ratios for all isotopomers of CO, HCO$^+$, and HOC$^+$ involving the nuclides ^{1}H, ^{2}H (D), ^{12}C, ^{13}C, ^{16}O, and ^{18}O. The ratios were obtained from unscaled vibrational frequencies computed at the CISD/6-31G** level (CISD/6-31G* for CO) and used to calculate equilibrium constants for isotope exchanges involving the reaction pairs HCO$^+$/CO, HOC$^+$/CO, and C$^+$/CO. Both simple proton transfers and more complex isotopic variants involving the breaking and reforming of CO bonds have been considered. The probable pathways for the HCO$^+$/CO and C$^+$/CO exchange reactions have been explored using higher accuracy quantum chemical calculations at the QCISD(T)/6-311G($2df$)//CISD/6-31G* level. The HCO$^+$/CO reaction proceeds through exothermic formation of the linear adduct OCHCO$^+$ with $D_{\infty h}$ symmetry. Similarly, the C$^+$/CO reaction proceeds along a spin-allowed pathway with exothermic formation of the linear adduct COC$^+$ with $D_{\infty h}$ symmetry. An alternate spin allowed pathway for the latter reaction passes through a pair of equivalent transition states with only C_s symmetry separated by a local minimum with C_{2v} symmetry.

[1] H. C. Urey, J. Chem. Soc. **1947**, 562.
[2] H. Craig, Geochim. Cosmochim. Acta **6**, 186 (1957); also see G. Faure, *Principles of Isotope Geology*, 2nd ed. (Wiley, New York, 1986), pp. 491–512.
[3] Y. Bottinga, J. Phys. Chem. **72**, 800 (1968).
[4] Y. Bottinga, Geochim. Cosmochim. Acta **33**, 49 (1969).
[5] Y. Bottinga, Earth Planet. Sci. Lett. **5**, 301 (1969).

J. Chem. Phys., Vol. 108, No. 19, 15 May 1998

Lawrence L. Lohr   8019

⁶Y. Bottinga and H. Craig, Earth Planet. Sci. Lett. **5**, 285 (1969).

⁷P. Richet, Y. Bottinga, and M. Javoy, Annu. Rev. Earth Planet Sci. **5**, 65 (1977).

⁸J. Bigeleisen, M. W. Lee, and F. Mandel, Annu. Rev. Phys. Chem. **24**, 407 (1973).

⁹W. D. Watson, Rev. Mod. Phys. **48**, 513 (1976); also see W. D. Watson, *Topics in Interstellar Matter*, edited by H. van Woerden (Reidel, Dordrecht, 1977), pp. 135–147; W. D. Watson, *Interstellar Molecules*, edited by B. H. Andrew (Reidel, Dordrecht, 1980), pp. 341–353.

¹⁰D. Smith and N. G. Adams, Astrophys. J. **242**, 424 (1980).

¹¹S. Wyckoff, E. Lindholm, P. A. Wehinger, B. A. Peterson, J.-M. Zucconi, and M. C. Festou, Astrophys. J. **339**, 488 (1989).

¹²G. J. White and G. Sandell, Astron. Astrophys. **299**, 179 (1995).

¹³S. J. Mojzsis, G. Arrhenius, K. D. McKeegan, T. M. Harrison, A. P. Nutman, and C. R. L. Friend, Nature (London) **384**, 55 (1996).

¹⁴D. S. McKay, E. K. Gibson, Jr., K. L. Thomas-Keprta, H. Vali, C. S. Romanek, S. J. Clemett, X. D. F. Chillier, C. R. Maechling, and R. N. Zare, Science **273**, 924 (1996); for different conclusions about the same Martian meteorite (ALH84001) see R. P. Harvey and H. Y. McSween, Jr., Nature (London) **382**, 49 (1996).

¹⁵C. H. Townes, *Topics in Interstellar Matter*, edited by H. van Woerden (Reidel, Dordrecht, 1977), pp. 113–123.

¹⁶P. G. Wannier, Annu. Rev. Astron. Astrophys. **18**, 399 (1980).

¹⁷E. Herbst and W. Klemperer, Astrophys. J. **185**, 505 (1973); **188**, 255 (1974).

¹⁸S. Green, Annu. Rev. Phys. Chem. **32**, 103 (1981).

¹⁹D. Smith and N. G. Adams, Int. Rev. Phys. Chem. **1**, 271 (1981).

²⁰H. W. Kroto, Int. Rev. Phys. Chem. **1**, 309 (1981).

²¹A. Dalgarno, J. Chem. Soc., Faraday Trans. **89**, 2111 (1993).

²²C. R. Cowley, *An Introduction to Cosmochemistry* (Cambridge University Press, Cambridge, 1995), pp. 125–149.

²³W. D. Langer and A. A. Penzias, Astrophys. J. **357**, 477 (1990); **408**, 539 (1993).

²⁴T. Xie, M. Allen, and W. D. Langer, Astrophys. J. **440**, 674 (1995).

²⁵R. P. A. Bettens and E. Herbst, Astrophys. J. **468**, 686 (1996); **478**, 585 (1997).

²⁶T. L. Wilson and R. T. Rood, Annu. Rev. Astron. Astrophys. **32**, 191 (1994).

²⁷B. E. Turner, Astrophys. J. **468**, 694 (1996).

²⁸GAUSSIAN 94, Revision B.3, M. J. Frisch, G. W. Trucks, H. B. Schlegel, P. M. W. Gill, B. G. Johnson, M. A. Robb, J. R. Cheeseman, T. Keith, G. A. Petersson, J. A. Montgomery, K. Raghavachari, M. A. Al-Laham, V. G. Zakrzewski, J. V. Ortiz, J. B. Foresman, C. Y. Peng, P. Y. Ayala, W. Chen, M. W. Wong, J. L. Andres, E. S. Replogle, R. Gomperts, R. L. Martin, D. J. Fox, J. S. Binkley, D. J. Defrees, J. Baker, J. P. Stewart, M. Head-Gordon, C. Gonzalez, and J. A. Pople (Gaussian, Inc., Pittsburgh, 1995).

²⁹A. J. Apponi and L. M. Ziurys, Astrophys. J. **481**, 800 (1997).

³⁰E. J. Bielske, S. A. Nizkorodov, F. R. Bennett, and J. P. Maier, J. Chem. Phys. **102**, 5152 (1995).

³¹N. N. Haese and R. C. Woods, Chem. Phys. Lett. **91**, 190 (1982).

³²R. G. A. R. Maclagan and P. Sudkeaw, J. Chem. Soc., Faraday Trans. **89**, 3325 (1993).

³³R. Flammang, Y. V. Haverbeke, M. W. Wong, A. Rühmann, and C. Wentrup, J. Phys. Chem. **98**, 4814 (1994).

³⁴Z. Cao and A. Tian, J. Mol. Struct.: THEOCHEM **334**, 45 (1995).